pubs.acs.org/Biomac

Article

Photodegradable Hydrogels for Rapid Screening, Isolation, and Genetic Characterization of Bacteria with Rare Phenotypes

Niloufar Fattahi,[▽] Priscila A. Nieves-Otero,[▽] Mohammadali Masigol, André J. van der Vlies, Reilly S. Jensen, Ryan R. Hansen,* and Thomas G. Platt*

Cite This: https://dx.doi.org/10.1021/acs.biomac.0c00543

Read Online

ACCESS | Metrics & More | Article Recommendations | Supporting Information

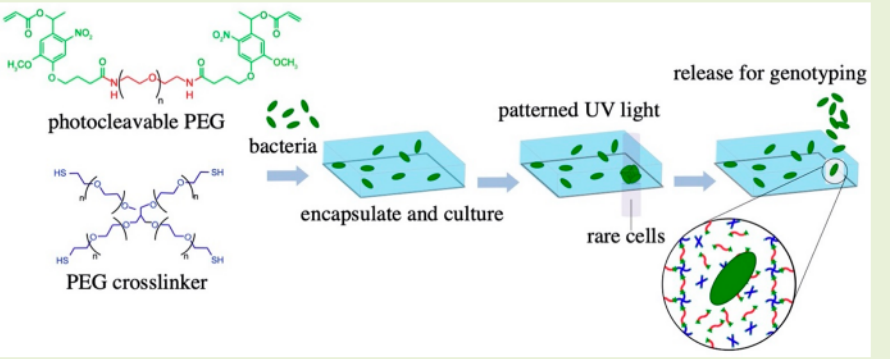

ABSTRACT: Screening mutant libraries (MLs) of bacteria for strains with specific phenotypes is often a slow and laborious process that requires assessment of tens of thousands of individual cell colonies after plating and culturing on solid media. In this report, we develop a three-dimensional, photodegradable hydrogel interface designed to dramatically improve the throughput of ML screening by combining high-density cell culture with precision extraction and the recovery of individual, microscale colonies for follow-up genetic and phenotypic characterization. ML populations are first added to a hydrogel precursor solution consisting of polyethylene glycol (PEG) *o*-nitrobenzyl diacrylate and PEG-tetrathiol macromers, where they become encapsulated into 13 μm thick hydrogel layers at a density of 90 cells/mm^2, enabling parallel monitoring of 2.8 × 10^4 mutants per hydrogel. Encapsulated cells remain confined within the elastic matrix during culture, allowing one to track individual cells that grow into small, stable microcolonies (45 ± 4 μm in diameter) over the course of 72 h. Colonies with rare growth profiles can then be identified, extracted, and recovered from the hydrogel in a sequential manner and with minimal damage using a high-resolution, 365 nm patterned light source. The light pattern can be varied to release motile cells, cellular aggregates, or microcolonies encapsulated in protective PEG coatings. To access the benefits of this approach for ML screening, an *Agrobacterium tumefaciens* C58 transposon ML was screened for rare, resistant mutants able to grow in the presence of cell free culture media from *Rhizobium rhizogenes* K84, a well-known inhibitor of C58 cell growth. Subsequent genomic analysis of rare cells (9/28,000) that developed into microcolonies identified that seven of the resistant strains had mutations in the *acc* locus of the Ti plasmid. These observations are consistent with past research demonstrating that the disruption of this locus confers resistance to agrocin 84, an inhibitory molecule produced by K84. The high-throughput nature of the screen allows the *A. tumefaciens* genome (approximately 5.6 Mbps) to be screened to saturation in a single experimental trial, compared to hundreds of platings required by conventional plating approaches. As a miniaturized version of the gold-standard plating assay, this materials-based approach offers a simple, inexpensive, and highly translational screening technique that does not require microfluidic devices or complex liquid handling steps. The approach is readily adaptable to other applications that require isolation and study of rare or phenotypically pure cell populations.

1. INTRODUCTION

The identification and isolation of microorganisms with rare or unique functions from heterogeneous populations is a critical step required to connect an organism's genotype with its phenotype.[1] These connections will enable researchers to gain a fundamental, predictive understanding of microbe function, to identify biomarkers that relate to specific diseases, and to engineer bacteria for applications in biotechnology. While phenotypic heterogeneity is prevalent in many microbial

Received: April 11, 2020
Revised: June 11, 2020
Published: June 19, 2020

Scheme 1. Overall Approach to Screening and Isolation of Rare Cells from Transposon Mutant Libraries[a]

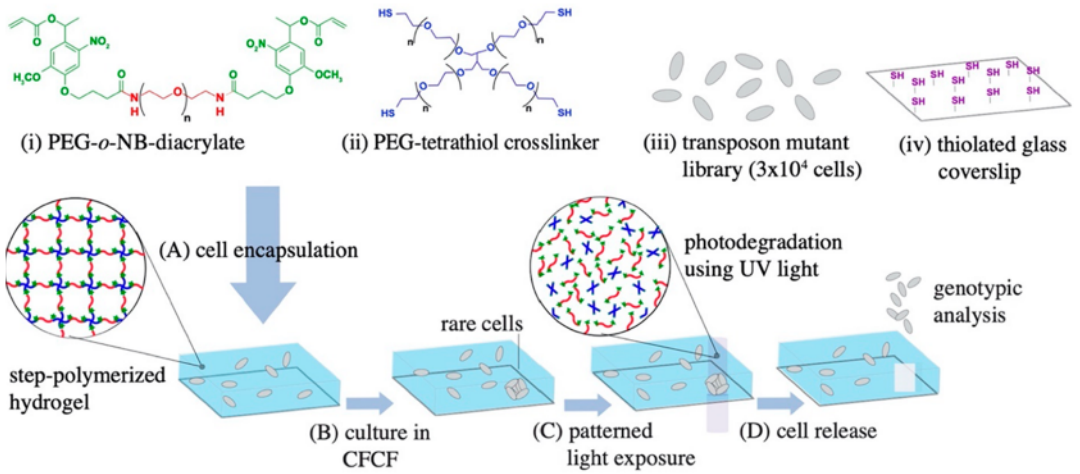

[a]Precursor materials consisting of (i) PEG-*o*-NB-diacrylate, (ii) PEG-tetrathiol crosslinker, (iii) a bacteria transposon mutant library, and (iv) a thiolated glass coverslip are prepared. (A) Precursor components are then mixed, resulting in the formation of a step-polymerized photodegradable hydrogel layer over the coverslip. (B) Cells are cultured in cell free culture fluid (CFCF) from an antagonistic species to identify mutants with rare growth profiles. (C) Patterned light is then used to spatially degrade portions of the hydrogel, (D) releasing resistant cells into solution for recovery and follow-up genotyping.

populations and communities, including among cells in populations that are genetically homogeneous or nearly homogeneous,[2,3] practical microbiological methods for screening and isolating phenotypically uniform groups of microbial cells are underdeveloped. This technical limitation poses a challenge to genotype-to-phenotype determination, which thus remains a broad knowledge gap in microbiology and biology more generally.[4]

Established methods of microbial cell isolation include flow-based sorting techniques such as fluorescence-activated cell sorting (FACS), which relies on a signal from fluorescently labeled proteins or fluorescence in situ hybridization probes to isolate cells with specific features from its environment.[5,6] FACS allows for high-throughput, single cell analysis capable of sorting of up to 50,000 cells per second.[7] However, subsequent cultivation and enrichment of recovered cells is often inhibited, as the labeling step compromises cell viability.[4] Further, FACS is limited by the inability to sort cells by time-dependent cellular properties.[8] Consequently, FACS is not directly amenable to growth-based screening. In addition, FACS is an impractical option for many laboratories due to its high cost (~$100−200/h) and availability often being limited to core research facilities. Motivated by these limitations, numerous micro- and nanoscale devices have been developed to isolate and study bacteria in recent years.[9−11] One common approach uses droplet-based microfluidic devices to partition cells into picoliter droplets, offering control over the chemical microenvironment and high-throughput, single cell analysis.[12] However, most devices have several limitations, a major one being that retrieval of individual cells from the device is difficult.[13] Ultimately, this inhibits follow-up genotyping and other -omics level characterizations after on-chip observation. These constraints impose a major limitation for screening and discovery applications. Recently, Lim et al. developed an innovative microwell platform for rapid screening of *E. coli* mutant libraries for mutants with growth rate differences,[14] demonstrating the benefits of off-chip recovery of individual cell populations for follow-up genotypic analysis. However, many micro- and nanoscale approaches require complex fabrication and liquid handling capabilities; thus, they often fail to translate into nonexpert microbiology laboratories.[4]

Hydrogel materials can provide an alternative strategy to microbe screening and isolation.[15,16] Here, individual cells from a suspension are encapsulated into an elastic, nanoporous hydrogel matrix, most commonly alginate or agarose, that facilitates diffusive biomolecular exchange.[17] Cells can then be cultured into high-density microcolonies, where enough biomass accumulates for cell preservation and follow-up characterization. Cells can be encapsulated into microscale hydrogel droplets using bulk emulsions[18] or 3D-bioprinters.[19] However, sorting and isolation of individual droplets containing a desired cell or cell population still remains a limitation and is most often achieved using FACS.[20] Photodegradable hydrogels enable an alternative mode of targeted cell recovery, thereby alleviating limitations associated with other hydrogel materials. Photodegradable hydrogels are designed to erode on exposure to light, enabling on-demand release of encapsulated cargo or manipulation of the biochemical and biophysical features of the microenvironment.[21] Because light can be patterned at single micron length scales, the approach affords a high level of spatial and temporal control over on-demand release.[22] This capability provides a distinct advantage for microbial selection and isolation applications in which specific cells must be released and retrieved from a screening interface with a high spatial precision. Recently, we reported the use of photodegradable hydrogels as a membrane to retrieve cell populations loaded and cultured in a microwell array format.[23] The hydrogel was generated by combining a poly(ethylene glycol)-*o*-nitrobenzyl diacrylate (PEG-*o*-NB-diacrylate) macromer with a four-arm PEG-thiol macromer, which generates a cross-linked PEG network through thiol−acrylate Michael-type addition reactions.[24] Using a patterned 365 nm light source, cell populations cultured in individual microwells can be released from wells and into solution on-demand and then plated and recovered.

https://dx.doi.org/10.1021/acs.biomac.0c00543
Biomacromolecules XXXX, XXX, XXX−XXX

Building off of these findings, here, we investigate the use of photodegradable hydrogels to screen and isolate phenotypically rare bacteria strains present in mutant libraries (MLs) for follow-up genotypic analysis (Scheme 1). The approach uses thiol−acrylate reactions to encapsulate a ML population into a three-dimensional PEG matrix over a thiolated glass coverslip. Encapsulated cells are cocultured in a defined media for screening, and individual cells with unique growth profiles are targeted for removal and downstream analysis. Each step in the screening procedure, including parallel growth monitoring of bacterial microcolonies, the effect of light pattern and exposure on the arrangement and viability of bacteria released from the hydrogels, and sequential extraction of multiple microcolonies, is developed toward high-throughput screening and recovery of viable cells. This enabled observation and recovery of any one of 3×10^4 mutants across a ∼310 mm^2 hydrogel area, a throughput that can accommodate enough mutant strains to rapidly screen even large bacterial genomes to saturation in a single assay (e.g., *Streptomyces* sp., genome of ∼8.7−11.9 Mbps,[25] requiring around 60,000 mutants to achieve saturation). This capability offers a significant reduction in the time and labor required to screen to saturation using standard plating techniques.

To demonstrate the benefits and feasibility of this approach, a ML of *Agrobacterium tumefaciens* C58 is screened for resistance to the antagonistic impacts of cell free culture fluid (CFCF) from *Rhizobium rhizogenes* K84. K84 produces multiple chemicals inhibiting the growth of C58, including the bacteriocin agrocin 84.[26,27] While C58 cells are susceptible to agrocin 84, rare mutations give rise to agrocin-resistant mutants. To identify these rare mutations, the phenotype of tens of thousands of mutants must first be evaluated. In a single test, we were able to screen, identify, and then isolate nine resistant C58 mutants from a ML containing ∼28,000 unique strains. Subsequent analysis of whole genome sequences identified mutations in the *acc* locus of the Ti plasmid conferring agrocin 84 resistance. This serves as the first example of a successful phenotype-to-genotype determination using this rapid screening approach.

2. EXPERIMENTAL SECTION

2.1. Materials. Pentaerythritol tetra (mercaptoethyl) polyoxyethylene (4 arm PEG, $((CH_2)_2{-}SH)_4$) was purchased from NOF America Corporation. PEG-diacrylate (PEGDA, MW 3400) was purchased from Laysan Bio. Fluorescein-5-maleimide was purchased from Cayman. Ethanol (EtOH), isopropanol, dimethylformamide (DMF), dichloromethane (CH_2Cl_2), diethyl ether (Et_2O), sodium hydrogen sulfate ($NaHSO_4$), anhydrous sodium sulfate (Na_2SO_4), and acetic acid (AcOH) were purchased from Fisher. D-(+)-Glucose, biotin ($C_{10}H_{16}N_2O_3S$), (3-mercaptopropyl) trimethoxysilane, sodium phosphate monobasic dihydrate ($NaH_2PO_4{\cdot}2H_2O$), sodium hydroxide (NaOH), alconox detergent, toluene anhydrous, *N*-hydroxysuccinimide (NHS), dicyclohexyl carbodiimide (DCC), PEG-diamine (MW 3400), deuterated chloroform ($CDCl_3$), phosphorpentoxide (P_4O_{10}), 4 Å molecular sieves, ninhydrin, and triethylamine (Et_3N) were purchased from Sigma-Aldrich. Silica TLC plates were from Merck. Ammonium sulfate ($(NH_4)_2SO_4$), magnesium sulfate heptahydrate ($MgSO_4{\cdot}7H_2O$), calcium chloride dihydrate ($CaCl_2{\cdot}2H_2O$), manganese(II) sulfate monohydrate ($MnSO_4{\cdot}H_2O$), kanamycin sulfate, spectinomycin sulfate, and iron(II) sulfate ($FeSO_4$) were purchased from VWR. DNeasy Blood & Tissue Kits were purchased from QIAGEN. The LIVE/DEAD BacLight Bacterial Viability Kit was purchased from ThermoFisher Scientific. All chemicals were used as received unless stated otherwise. 4 Å molecular sieves were heated under vacuum at 200 °C for 4 h to remove water. CH_2Cl_2 was dried with 4 Å molecular sieves. Et_3N was distilled from ninhydrin at atmospheric pressure and stored over KOH pellets. NHS, DCC, and PEG-diamine were dried under vacuum in the presence of P_4O_{10} at 40 °C for 19 h. NB-COOH (see Scheme S1 for the chemical structure) was prepared as previously reported.[16] The ninhydrin staining solution was prepared by dissolving 300 mg of ninhydrin in 97 mL of EtOH and 3 mL of AcOH and stored in the dark.

2.2. Synthesis of the Photodegradable Poly(ethyleneglycol) Diacrylate. PEG-*o*-NB-diacrylate was prepared with slight modifications from that previously reported[23] and is shown in Scheme S1. 519 mg (1.5 mmol) of NB-COOH and 175 mg (1.5 mmol) of NHS were dissolved in 4 mL of DMF and 8 mL of CH_2Cl_2. The clear solution was cooled on ice for 15 min, and a solution of 304 mg (1.5 mmol) of DCC in 2 mL of CH_2Cl_2 was added dropwise over the course of 5 min. After stirring for 21 h at room temperature, a solution of 508 mg (0.15 mmol, 0.30 mmol NH_2 groups) of PEG-diamine and 51 μL (0.37 mmol) of Et_3N in 9 mL of CH_2Cl_2 was added dropwise over the course of 10 min to the turbid reaction mixture. After stirring for 20 h, spotting of the reaction mixture on a silica TLC plate followed by ninhydrin staining and heating showed the absence of amine groups. The mixture was concentrated in a flow of nitrogen to remove CH_2Cl_2, and the residue was diluted with 16 mL of 1 M $NaHSO_4$ (aq). The suspension was passed through a glass filter, and the white residue was washed with 9 mL of 1 M $NaHSO_4$ (aq). The slightly hazy filtrate was then passed through a syringe filter (0.45 μm). After the syringe filter was washed with 1 M $NaHSO_4$, the clear yellow filtrate (30 mL) was extracted with CH_2Cl_2 (5 × 30 mL). The extracts were combined, dried over Na_2SO_4, filtered through Whatman paper, and concentrated under reduced pressure at 30 °C. The oily residue was dissolved in 8 mL of CH_2Cl_2, and the solution was slowly diluted by adding 200 mL of Et_2O. The precipitate was collected on a glass filter, washed with Et_2O (3 × 10 mL), and dried. This Et_2O precipitation was repeated one more time to yield PEG-*o*-NB-diacrylate (539 mg) as a light-yellow solid. ^{1}H NMR ($CDCl_3$) δ 7.58 (s, CH_{aromat}), 7.00 (s, 1H, CH_{aromat}), 6.52 (m, CH), 6.45 (bs, NH), 6.44 (d, $CH{=}CH_{trans}$), 6.16 (dd, $CH{=}CH_2$), 5.87 (d, $CH{=}CH_{cis}$), 4.10 (t, $CH_2CH_2CH_2O$), 3.92 (s, OCH_3), 4.22−3.20 (CH_2CH_2O + OCH_2CH_2N), 2.39 (t, CH_2CO), 2.17 (m, $CH_2CH_2CH_2$), 1.65 (d, CH_3CH). The degree of functionalization using MW = 3400 was 80% by comparing the integral ratios of the aromatic and CH_2CH_2O PEG protons. The ^{1}H NMR spectrum is shown in Figure S1. ^{1}H NMR spectra were measured on a Varian System 500 MHz spectrometer in deuterated chloroform ($CDCl_3$). A total of 32 scans was collected, and the D1 was set to 10 s. Chemical shifts (δ) are reported in ppm and are referenced against the residual $CHCl_3$ peak at 7.26 ppm.

2.3. Bacterial Strains and Culture Conditions. All strains and plasmids used in this study are described in Table S1. Wildtype *A. tumefaciens* C58 (herein referred to as C58) was used for the live/dead assay. *A. tumefaciens* C58 cells constitutively expressing the fluorescent protein GFPmut3 (herein referred to as C58-GFP) were used as controls in the hydrogel experiments. Populations of fluorescent *A. tumefaciens* C58-GFP *Himar1* mutant library cells (described below and herein referred to as C58 ML) were used in seeding, culture, and screening experiments within the hydrogels. *A. tumefaciens* strain NT1 was used as an agrocin 84 resistant control in the agrocin 84 bioassay. Unless noted otherwise, the *A. tumefaciens* strains were grown on AT minimal medium[28] supplemented with 0.5% (w/v) glucose and 15 mM ammonium sulfate (ATGN). *Rhizobium rhizogenes* strain K84 (herein referred to as K84) bacterial cells were cultured in suspension at 28 °C (215 rpm) for 24−48 h to reach an OD_{600} of 0.7 in ATGN media supplemented with kanamycin (150 μg/mL), spectinomycin (100 μg/mL), biotin (2 μg/mL), and iron as Fe (II) sulfate (0.022 mM).

The optical densities of bacteria cultures (100 μL) at 600 nm (OD_{600}) were measured using an Epoch2 microplate reader (Biotek) in 96-well plates for all experiments. After K84 reached an OD_{600} of 0.7, the bacterial culture was centrifuged at 2000*g* for 10 min and the supernatant containing cell free culture fluid (CFCF) from K84 was

https://dx.doi.org/10.1021/acs.biomac.0c00543
Biomacromolecules XXXX, XXX, XXX−XXX

sterile filtered two times, first with a 0.45 μm syringe filter and a second time with a 0.2 μm syringe filter, before being used in screening experiments.

2.4. Transposon Mutagenesis. The *mariner* transposon *Himar1* was used to mutagenize C58-GFP cells using previously described methods.[29] In brief, *E. coli* S17-1/λpir pFD1 and C58-GFP cells were mixed and incubated overnight at 28 °C on a 0.2 μm polyethersulfone (PES) disk filter (PALL) placed on a LB plate. Following incubation, cells were collected and frozen at −80 °C in 25% glycerol.

2.5. Media for Screening Experiments. 8× ATGN media was prepared as the undiluted base media. For unconditioned media, 8× ATGN was diluted to 1× with sterile ultrapure water and then supplemented with iron (0.022 mM), biotin (2 μg/mL), kanamycin (150 μg/mL), and spectinomycin (100 μg/mL). For conditioned media, 8X ATGN was diluted with the CFCF acquired from K84 (section 2.3) to get 1× ATGN that was subsequently supplemented with iron (0.022 mM), biotin (2 μg/mL), kanamycin (150 μg/mL), and spectinomycin (100 μg/mL).

2.6. Thiol Surface Functionalization. Thiol functionalized surfaces can be used as a route for secondary surface modifications through thiol−acrylate addition reactions[30] and are used here to provide covalent attachment of the hydrogel to the coverslip surface. Glass coverslips (1.8 × 1.8 cm) were cleaned with oxygen plasma for 3 min using a PDC-001-HGP Plasma Cleaner (Harrick Plasma). Coverslips were then cleaned and hydroxylated in Piranha solution, a 30:70 (v/v) mixture of H_2O_2 and H_2SO_4, at 60−80 °C for 30 min.[31] (*Caution! Strongly corrosive.*) Coverslips were then rinsed and stored in ultrapure water at room temperature. For functionalization with thiol groups, coverslips were then dried under a N_2 stream and immersed into a 269 mM (3-mercaptopropyl) trimethoxysilane (MPTS) solution in dry toluene (5 v/v) for 4 h at room temperature. Substrates were then rinsed with toluene, ethanol/toluene (1:1), and ethanol, 4 times each.[31] They were then dried under a N_2 stream and stored at 4 °C for further use.

2.7. Hydrogel Preparation and Growth Monitoring. All hydrogels were made in 1× ATGN phosphate buffer, pH 8. This was made by first adding NaH_2PO_4 to 2× ATGN and adjusting to pH 8 using 5 M NaOH (aq); the solution was then sterile filtered and stored at −20 °C until further use. Bacteria were encapsulated into the hydrogels by first inoculating 1 mL of 2× ATGN media with 2 μL of cells from the 25% glycerol stock stored frozen at −80 °C, for both the C58 ML and the C58-GFP control. This resulted in a C58 ML concentration of 3.63 × 10^7 CFU/mL in 1× ATGN media, pH 8. Then, a hydrogel precursor solution was prepared by adding photodegradable PEGDA (M_n 3400 Da, 8.4 μL, 49 mM) in water into 18.75 μL of the inoculated ATGN. Lastly, PEG-tetrathiol (M_n 10 000 Da, 10.35 μL, 20 mM) in water was added to the mixture, resulting in an equimolar acrylate−thiol ratio. The concentrations of acrylate and thiol groups in the final solution were each 22 mM. The final solution volume was 37.5 μL.

The cell suspension was added to a thiol-functionalized coverslip (Section 2.6) to allow for covalent attachment of the hydrogel to the glass surface through thiol−acrylate addition (Scheme S2). First, 7 μL of the cell suspension was pipetted onto a chemically inert perfluoroalkylated glass slides, made as previously reported.[23] This coverslip was then contacted with the thiolated coverslip, separated by a fixed distance of 12.7 μm using Stainless Steel Thickness Gage Blades (Precision Brand). The solution was incubated for 25 min at room temperature to allow for cross-linking of the PEG polymers and hydrogel formation. After gelation, the thiolated glass slide and attached hydrogel were gently removed from the perfluoroalkylated glass slide. Care was taken during this step to prevent the hydrogel from rupturing. With these conditions, it was noted that spacers thicker than 12.7 μm resulted in an overlay of cells, which was not desired because cell colonies above or beneath the target colony are also released during light exposure, which may result in cross-contamination during cell retrieval (Figure S2). For screening experiments, hydrogels were placed in 60 × 15 mm Petri dishes and cultured in ATGN media or ATGN/CFCF media in an incubator at 28 °C. For growth monitoring, cells were cultured in ATGN media at 28 °C in a live cell incubation chamber (Tokai Hit) placed over a Nikon Eclipse Ti-E inverted fluorescence microscope. Time lapse fluorescence images of the bacteria during growth into microcolonies within the hydrogel were taken with a 10×, NA 0.3 or 20×, NA 0.45 lens using NIS-Element software. Growth rates were quantified using Growthcurver software.[32]

2.8. Hydrogel Degradation and Cell Release with the Polygon400 Light Patterning Device. Hydrogels were exposed to various patterns of UV light from a 365 nm LED light source using the Polygon400 patterned illumination tool (Mightex Systems) configured to an Olympus BX51 upright microscope. The tool exposes 365 nm light at micron-scale resolution across a user-defined area for a given exposure time, enabling spatiotemporal control of hydrogel degradation (Figure S3). Intensity of the 365 nm irradiated light was controlled using Mightex PolyScan2 software and varied between 0.7 and 7 mW/mm^2. Prior to hydrogel degradation, the tool was calibrated to the specific objective using a mirror and the calibration software to obtain a clean and sharp pattern exposed on the mirror with the selected objective. Hydrogels were then placed in a PDMS holder and covered with ATGN media to prevent the hydrogel from dehydration (Figure S4). Targeted microcolonies were identified with the microscope and then focused on within the three-dimensional hydrogel. This focusing step was important to maintain a sharp UV exposure pattern over the targeted cells, as regions above and below the focused region of the hydrogel become exposed to out of focus UV light, causing the degradation pattern to become scattered in these regions. This is an inherent limitation of the upright microscope. Exposure occurred with a 10×, NA 0.3 or 20×, NA 0.5 objective. Brightfield images and movies were taken during photodegradation using Infinity Capture Software.

2.9. Labeling the Hydrogel with Fluorescent Dye. Fluorescence microscopy was used to image the hydrogel after UV light exposure and degradation by labeling with fluorescein-5-maleimide, which couples to pendant thiol groups within the hydrogel.[33] 4 μL of a 10 mM stock solution of fluorescein maleimide in DMF was added to 1 mL of PBS buffer (pH 7.3) and then added to the hydrogel for 2 h at room temperature in a dark environment. The hydrogel was then rinsed with 1× PBS to remove unbound fluorophores and imaged.

2.10. Live/Dead Assay. To investigate cell viability after exposure of microcolonies to UV light, a live/dead assay was used. Here, C58 cells were encapsulated in hydrogels containing nonphotodegradable PEGDA (M_n = 3400 Da) instead of PEG-*o*-NB-diacrylate; thus, colonies remained within the hydrogel after UV exposure for staining and imaging. The stain mixture was prepared as recommended by the manufacturer. 300 μL of the mixture was added over each hydrogel and incubated in the dark for 15 min. SYTO 9 labels both intact and compromised cells, while propidium iodide labels only cells with damaged membranes, resulting in the reduction of expressed fluorescence by SYTO 9.[34] After staining, the hydrogels were washed thoroughly with a 0.85 wt % NaCl solution and imaged using the inverted fluorescence microscope. The percentage of live cells (p) was estimated from the fluorescence intensity data according to eq 1:

$$p = 100 - \left(\frac{r_{UV} - r}{r_{dead} - r}\right) \times 100 \quad (1)$$

where r_{UV} is the measured red signal following UV exposure, r is the red signal measured when the hydrogel is not exposed to UV, and r_{dead} is the red signal of the dead cell control. For this control, cells were killed by incubating the hydrogel in 70% isopropanol at room temperature for 20 min. The hydrogel was then washed with ultrapure water before staining.

2.11. Cell Retrieval and Recovery. Immediately after light exposure, the free end of a 20 cm long PTFE tubing, 0.05 in. ID, was placed over the irradiated spot. The other end was attached to a 100 μL syringe that was used three times to aspirate the media containing the released cells. For every exposed microcolony, 300 μL of solution was collected and transferred into an Eppendorf tube. For each sequential microcolony extracted, the syringe, tubing, PDMS holder, and the hydrogel were washed with ultrapure water at least 3 times to

https://dx.doi.org/10.1021/acs.biomac.0c00543
Biomacromolecules XXXX, XXX, XXX−XXX

minimize cross-contamination. Following cell retrieval, 300 μL of the bacterial solution was plated onto selective media for recovery. The plating process was also expected to dilute PEG degredation biproducts. 100 μL of the solution was plated on ATGN supplemented with kanamycin and spectinomycin. Cells from the mutant library are expected to be resistant to both antibiotics. In contrast, C58-GFP, the parental strain used to generate the mutant library, is resistant only to spectinomycin. The presence of both antibiotics allowed for the recovery of mutants, decreasing the chance of contamination from other sources. After inoculation, the plates were incubated at 28 °C for 3 to 5 days.

2.12. Agrocin 84 Bioassay. Agrocin 84 bioassays were performed to determine if recovered mutants are resistant to agrocin 84, a bacteriocin produced by K84 that strongly antagonizes C58. The bioassay protocols were adapted from those reported by Hayman et al.[35,36] K84 and recovered C58 ML mutants (Section 2.11) were grown in liquid ATGN as previously described for 24 h. All cultures were normalized to an OD_{600} of 0.6 in ATGN media. Tubes containing 10 mL of molten agar (65 °C) were inoculated with 35 μL of the C58 mutant cultures. The tubes were vortexed vigorously for 10 s and then poured onto sterile 60 × 15 mm Petri dishes. Once the agar solidified, 7.5 μL of the K84 cells (OD_{600} = 0.6) was spotted in the center of the plate and allowed to air-dry. Once the K84 cells had dried completely, the plates were wrapped with a plastic wrap to prevent drying of the media, and they were incubated at 28 °C for 72 to 120 h.

2.13. Genomic DNA Purification. QIAGEN's DNeasy Blood & Tissue Kit was used to purify bacterial genomic DNA from cellular debris and any residual PEG byproduct. The manufacturer's protocol, including the Gram-negative bacteria pretreatment, was followed with minor modifications. Proteinase K incubation was performed for 60 min at 56 °C, and 4 μL of RNase A (100 mg/mL) was added following proteinase K incubation. Lastly, two sequential elution steps via centrifugation were included: the first elution used 150 μL of Buffer AE while 50 μL of Buffer AE was used for the second elution. Genomic DNA samples were stored at −20 °C.

2.14. Whole Genome Sequencing. Genomic DNA samples were sent to the Microbial Genomic Sequencing Center (MiGS) in Pittsburgh, PA. Samples were received and immediately frozen until the library preparation began. Qubit fluorometric quantification was used to quantify DNA concentrations. All samples were normalized to the same concentration and enzymatically fragmented using an Illumina tagmentation enzyme. Unique indices were attached to each pool of fragmented genomic DNA using PCR, and the resulting barcoded pools were combined to multiplex on an Illumina NextSeq 550 flow cell.

2.15. Sequence Analysis. Bioinformatic analyses were performed on Beocat, the High-Performance Computing cluster at Kansas State University. Once sequencing reads were acquired from the MiGS, read mapping was performed by aligning the reads to the C58 reference genome using the Burrows-Wheeler Aligner's Smith-Waterman Alignment (BWA-SW) algorithm.[37] The BWA-SW algorithm aligns long sequences (up to 1 Mb) against a large reference genome in a fast and accurate manner. A variant calling applying the Genome Analysis Toolkit (GATK) was then applied. GATK is a pipeline that compares the alignment of our reads to the C58 genome at a more detailed level while simultaneously performing a base quality score recalibration, indel realignment, duplicate removal, and SNP and INDEL discovery.[38] Additionally, the GATK pipeline applies standard hard filtering parameters or variant quality score recalibration that result in the identification of mutations with high confidence. The purpose of the read mapping and variant calling is to find the mutation responsible for agrocin 84 resistance. Once the mapped reads and the variants were generated, regions with mutations were identified.

3. RESULTS AND DISCUSSION

3.1. High Density Cell Encapsulation and Parallel Tracking of Cell Growth. The first step in developing the hydrogel interface involved achieving high-density encapsulation of viable bacteria cells within the hydrogel for growth monitoring. C58 ML cells were seeded across a 1.8 × 1.8 cm glass coated with a hydrogel, initially 12.7 μm thick, that reached 140 μm in its swollen state after incubation. Given the genome size of *A. tumefaciens* C58 (approximately 5.67 Mbps),[39] the observation of 28,000 mutants within a single hydrogel was desired to ensure that the genome could be screened to saturation with 99% certainty.[40] Using fluorescence microscopy, it was found that seeding bacteria at a concentration of 3.63×10^7 CFU/mL encapsulated bacteria at a density of 90 CFU/mm^2, meeting this requirement. As shown in Figure 1A, after encapsulation, cells appeared

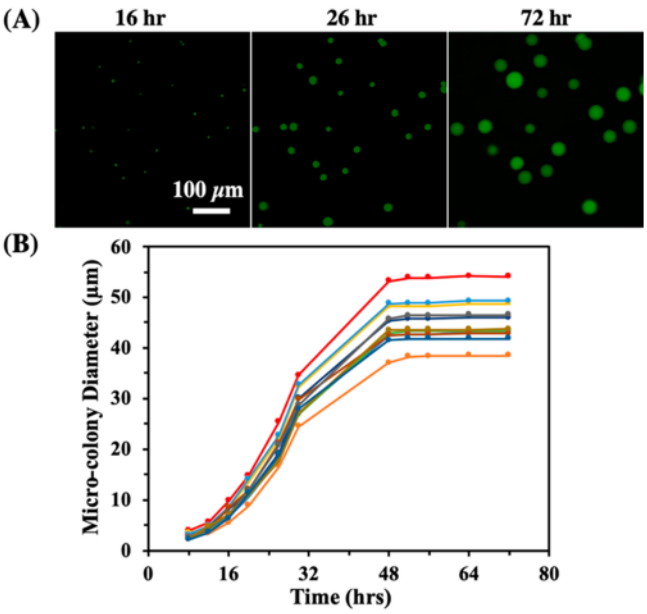

Figure 1. Parallel growth monitoring of individual C58 cells into microcolonies within the hydrogel matrix after seeding. (A) Representative fluorescence images of C58 ML microcolonies at different time points. (B) Microcolony growth for 11 sample microcolonies within the hydrogel as a function of time.

randomly dispersed and the vertical overlap of cells was minimal, which was desired to prevent the extraction of multiple colonies during the light exposure step. Hydrogel thicknesses greater than 12.7 μm resulted in the vertical overlap of cells (Figure S2).

After encapsulation, parallel growth tracking of individual cells into microcolonies during culture in ATGN media was achieved. Microcolonies become visible under 20× magnification, 8 h after encapsulation. They then grow (k = 0.18 h^{-1}) in diameter for approximately 40 h (Figure 1B). These observations suggest that there was sufficient mass transfer to support cell growth. Hydrogel mesh size (ξ), a critical determinant of mass transfer within the hydrogel,[41] was calculated to be 10 nm on the basis of the equation described by Canal and Peppas,[42] small enough for the immobilization of bacteria cells but large enough for the diffusive exchange of nutrients (e.g., glucose) and waste products. Similar growth trajectories were observed when monitoring the growth of free cells in a 96-well plater reader (Figure S5), suggesting that cell confinement or diffusion limitations had a minimal effect on growth within the hydrogel environment. Cells developed into spherical microcolonies due to deformation of the elastic PEG

https://dx.doi.org/10.1021/acs.biomac.0c00543
Biomacromolecules XXXX, XXX, XXX−XXX

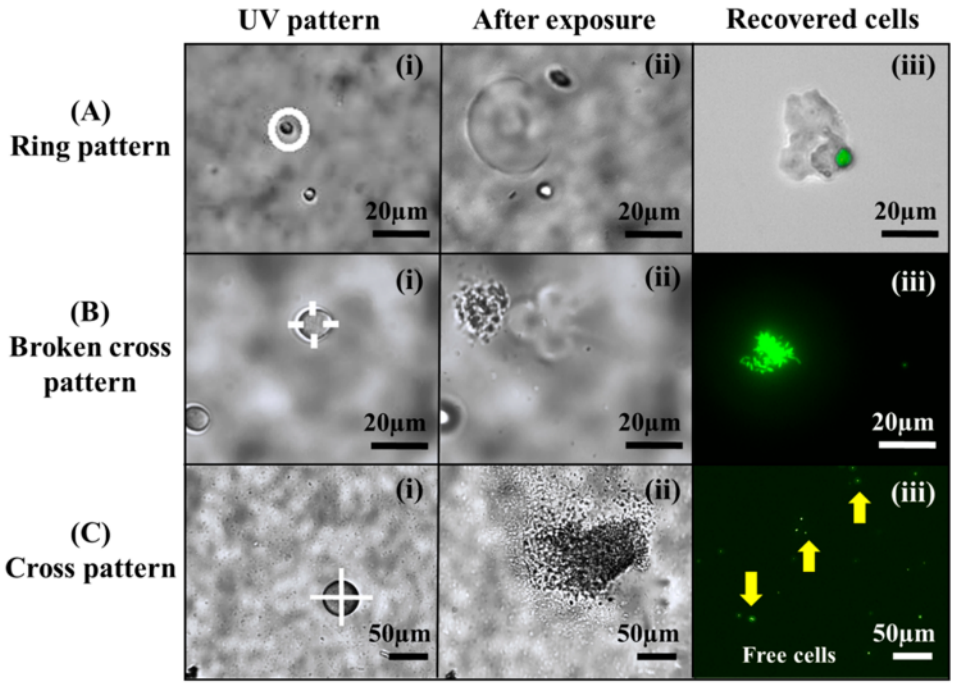

Figure 2. C58 ML cell arrangement after release with different light patterns. (A) Ring pattern for the extraction of colonies protected within a PEG layer. (B) Broken cross pattern for the extraction of aggregated cells. (C) Cross pattern for the extraction of predominantly free cells. For each exposure pattern, the following are shown: (i) the projected light pattern (white line) over a targeted colony, (ii) the hydrogel immediately after cell release, and (iii) brightfield and/or fluorescence images of the recovered cells in solution. Patterns were exposed at an intensity of 4.2 mW/mm^2.

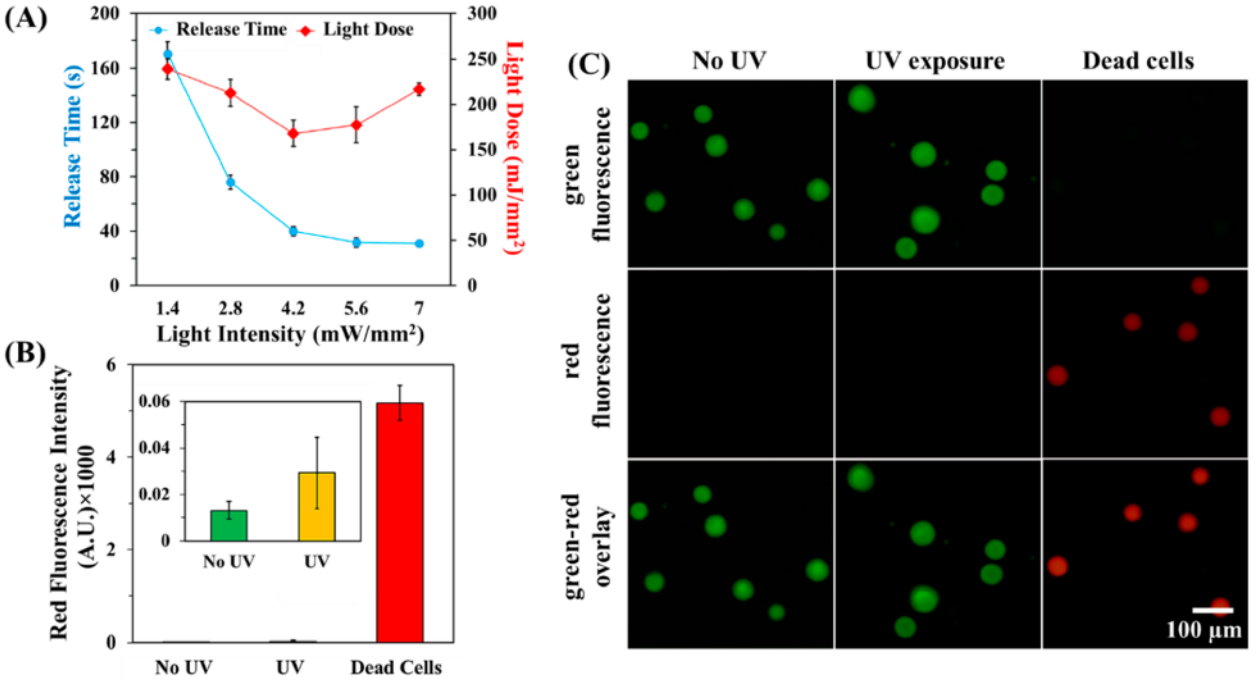

Figure 3. (A) Microcolony release time from hydrogels at varied 365 nm light intensity. An entire cell mass lift off effect was noted during broken cross pattern exposure, providing a discrete time point for cell release. (B) Red fluorescence signal after staining with the reagents in the live/dead bacterial viability kit. Microcolonies without UV exposure, with broken cross pattern UV exposure (4.2 mW/mm^2, 40 s), and from chemically treated (70% isopropanol) dead cells are compared. (C) Representative green-red fluorescence images of microcolonies after staining with the live/dead assay. Dead cells with compromised membranes appeared red. ImageJ software was used to adjust the images for color contrast. For each treatment (n = 3 independent trials), 30 different microcolonies were imaged.

matrix caused by the local increase in cell numbers and through chemical or enzymatic modes of hydrogel degradation.[43] These measurements were performed several times (n = 26) with 92% of the trials resulting in microcolony growth. At

https://dx.doi.org/10.1021/acs.biomac.0c00543
Biomacromolecules XXXX, XXX, XXX−XXX

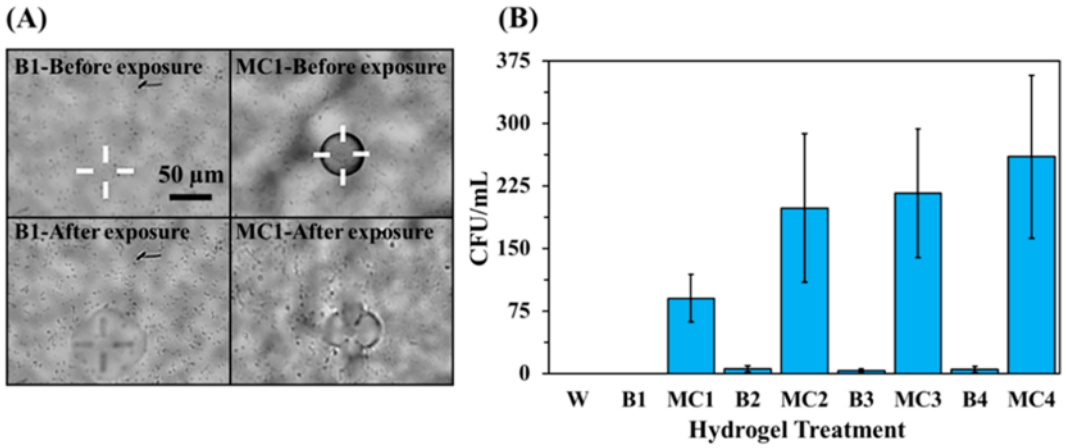

Figure 4. Sequential extraction of targeted microcolonies from a hydrogel. (A) Brightfield image of a hydrogel with a sample exposure map (white lines) showing exposure locations targeting a blank area or a microcolony with a broken cross pattern. (B) Colony forming units (CFU/mL) of recovered suspensions after washing the hydrogel at various steps and plating. W = initial wash of the hydrogel; B = hydrogel blank; MC = microcolony. All exposures, wash steps, and plating steps onto selective media were performed under identical conditions (n = 3 independent trials).

later time points (~5 days), bacteria were observed to escape hydrogel encapsulation (Figure S6A). While chemical hydrolysis of thioether−ester linkages may play a role in hydrogel degredation,[44] follow-up studies have indicated that hydrogels remain capable of immobilizing inert, 1 μm fluorescent beads at neutral pH over 5 days (Figure S6B,C). Others have also reported minimal mass loss in similar thiol−acrylate PEG hydrogels over a 5 day time period at neutral pH.[45] These observations suggest that bacteria within the microcolonies were the cause of the eventual breakdown of the hydrogel matrix.

3.2. Characterization of Cell Release and Cell Viability. Using light for extraction has the advantage of spatiotemporal control of cell release, as the patterned illumination tool allows for projection of user-defined, two-dimensional patterns over any microcolony within the hydrogel. Here, the arrangement of cells released into solution after exposure with different patterns was investigated. Microscale patterns including lines, rings that outline the microcolony perimeter, a cross, or a broken cross pattern were investigated. Patterns with greater coverage of the colony such as circles were avoided to minimize unnecessary UV light exposure in an effort to preserve bacteria viability and DNA quality. The recovered cells present in the extract solution were then imaged in brightfield and fluorescence modes to examine the cell arrangement (Figure 2).

Light patterning offered control of the arrangement for cells liberated from the hydrogel interface. Ring patterns degraded the hydrogel immediately surrounding the microcolony, forming a hydrogel island that immediately detached from the interface (Supplementary Movie 1). Examination of the extract solution revealed that cells remained encapsulated as microcolonies in the detached hydrogel (Figure 2Aiii). This pattern offers the advantage that extracted cells are not directly exposed to UV light and that they remain preserved in a larger, protective PEG layer, being potentially useful for downstream separation or processing steps. Cross patterns instead appeared to liberate cells as either aggregates or free cells (Figure 2Biii,Ciii), as these exposure patterns etched a direct path for cellular transport out of the hydrogel. Here, it was noted that the entire cell mass was liberated into the media covering the hydrogel as the membrane became compromised (Supplementary Movie 2 and Figure S7). Inspection of the recovered cells in the extract solution revealed that broken cross patterns favored aggregated cells, whereas cross patterns contained extract solutions dominated by free cells. Other patterns, such as individual lines patterned at the microcolony edge, also caused a burst of free cells into solution (Supplementary Movie 3); however, some of the cells appeared to remain in the hydrogel after exposure (Figure S7). Because removal of a maximum number of target cells with a minimum direct exposure to UV light was desired, the broken cross pattern was selected for further use.

After establishing that using broken cross pattern exposure results in lift off of the entire cell mass, we investigated how varied light intensities affected release time, defined here as the exposure time until microcolony burst is observed (Figure 3A). Step growth hydrogels are characterized by rapid erosion rates due to the low levels of network connectivity;[24] here, degradation and cell release were noted in <180 s for all exposure intensities studied. Cell release time showed significant decreases with increasing light intensity up to an intensity of 4.2 mW/mm^2 ($P < 0.05$); this trend was expected as exposure time required for reverse gelation of the hydrogel is inversely proportional to light intensity.[24] Beyond this, only minor decreases in release time were noted and a minimum light dose for release was found at 168 ± 14 mJ/mm^2, corresponding to an intensity of 4.2 mW/mm^2.

Since 365 nm light can be cytotoxic to bacteria through the generation of reactive oxygen species,[46] the effect of broken cross pattern exposure (4.2 mW/mm^2, 40 s) on cell viability was characterized using a live/dead assay (Figure 3B,C). Here, C58 cells were first seeded within a hydrogel generated with PEG diacrylate without the photocleavable o-NB moiety and cultured into microcolonies, and the colonies were then exposed to broken cross patterns of light. Removal of the o-NB group from the network backbone ensured that the microcolonies would remain in place during exposure so they could be subsequently stained and observed with fluorescence microscopy. The comparison of red signal indicating nonviable cells showed no significant difference between unexposed and exposed cells, both of which were significantly less than the

https://dx.doi.org/10.1021/acs.biomac.0c00543
Biomacromolecules XXXX, XXX, XXX−XXX

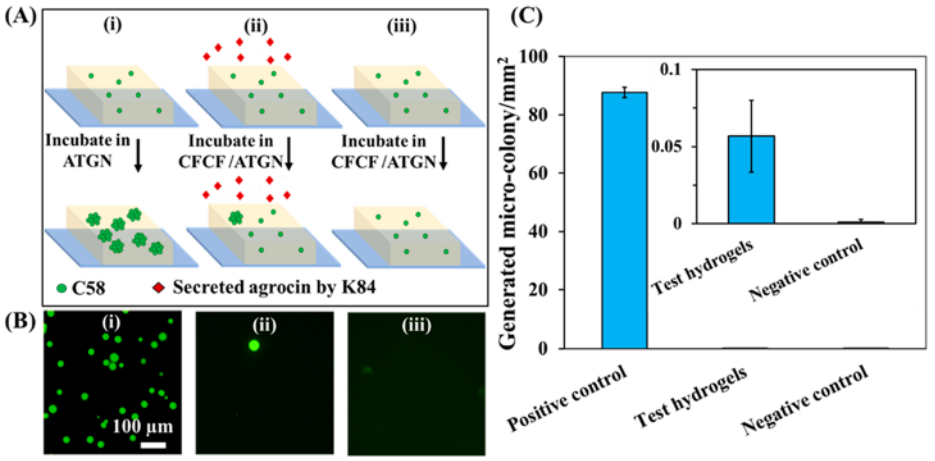

Figure 5. (A) Schematic of the ML screen. (i) Positive control: growth of C58 ML cells within the hydrogel; (ii) hydrogel incubation in the presence of CFCF/ATGN for growth of agrocin resistant C58 ML cells; (iii) negative control: C58-GFP incubated in CFCF/ATGN under identical conditions. (B) Representative fluorescence images of the fluorescent microcolonies in the (i) positive control, (ii) test hydrogels, and (iii) negative control. (C) Representative data for generated microcolonies in each treatment (n = 3 independent trials).

dead cell control ($P < 0.01$). This suggests that the majority of cells remain viable during the extraction step for recovery and genomic analysis. Given these findings, these exposure conditions were used in the remaining studies.

3.3. Sequential Extraction and Recovery of Individual Microcolonies. Isolation of bacteria for pure cultures is one of the most important requirements in microbiological techniques because it enables extraction of pure genetic material, allows for follow-up biological and biochemical testing, and eliminates confounding observations that can arise from other bacteria. Here, the ability to generate pure cultures exclusively from the bacteria targeted for extraction was evaluated. Hydrogels were first seeded and cultured for microcolony development and placed inside a PDMS holder (Figure S4). Designated areas of the hydrogel were exposed to UV light and then immediately washed with wash buffer to remove the released cells. Wash solutions were plated on selective media to quantify colony forming units (CFU/mL) in each wash solution. To verify the presence or absence of contaminating bacteria in the media prior to extraction, hydrogels were initially washed prior to light exposure. Additionally, as a negative control, areas of the hydrogel where no colonies were present were exposed to UV light under the same conditions used for cell release. This was done before and after every microcolony extraction, and washes from these blank areas were processed and plated in an identical manner as those solutions containing an extracted microcolony. In this way, carryover and cross-contamination during subsequent microcolony extraction could be identified. Using this approach, the purity of four sequentially extracted microcolonies was accessed (Figure 4).

The initial washings of the hydrogels and negative controls generated from the opening of the hydrogel in areas lacking colonies showed little or no recovery after plating (Figure 4B). Conversely, solutions extracted from selected microcolonies showed significant growth after plating, with average measurements ranging from 90 ± 28 CFU/mL (MC1) to 260 ± 98 CFU/mL (MC4). The number of cells (CFU/mL) in the wash buffer after microcolony extraction showed no significant association with microcolony size (Figure S8). A small amount of carryover (<5 CFU/mL) was noted in blank solutions after the first microcolony extraction, suggesting that cross-contamination from a previously opened microcolony is a possibility during sequential extraction; however, these levels were minimal, representing <1% of cells recovered from a typical microcolony. These observations demonstrate that the extraction method allows for targeted and clean recovery of bacteria colonies, enabling one to sample and isolate multiple colonies from a single screen, if desired.

3.4. Screening and Identification of Rare Phenotypes from Transposon Mutant Libraries. Following the characterizations in Sections 3.1 to 3.3, the photodegradable hydrogels were evaluated for use in a model ML screening application. The screen involved seeding and culturing C58 ML cells in media supplemented with cell free culture fluid (CFCF) from K84, which contains agrocin 84, a well-known bacteriocin with activity against C58.[26,27] During this screen, three separate hydrogels were prepared from the same hydrogel precursor solution. This included a positive control where C58 ML cells were incubated in liquid ATGN (as in Section 3.1) to ensure normal cell growth across the population (Figure 5Ai). This control also allowed for verification that seeding density remained consistent with previous experiments (approximately 90 CFU/mm^2). To quantify the total number of bacteria cells that were screened in any trial, 10 separate areas on the positive control hydrogels were imaged. As a negative control, C58-GFP was also cultured in ATGN/CFCF, where no growth was expected (Figure 5Aiii), verifying that an inhibitory environment for normal cell growth was present. With these two controls in place, mutants within the seeded ML population that were able to grow in the presence of ATGN/CFCF were identified as candidate agrocin 84 resistant mutants (Figure 5Aii).

Once each cell population was encapsulated in the respective hydrogels, they were immersed in ATGN or ATGN/CFCF media, incubated, and then imaged using fluorescence microscopy. ML cells seeded in positive control hydrogels consistently grew into fluorescent microcolonies (Figure 5Bi) at 28 °C within 24 h, as expected. C58 ML cells in the positive control were quantified at a density of 90 cells/mm^2, indicating that approximately 28,000 cells were present within the hydrogel. Test hydrogels were immersed in ATGN/CFCF

https://dx.doi.org/10.1021/acs.biomac.0c00543
Biomacromolecules XXXX, XXX, XXX−XXX

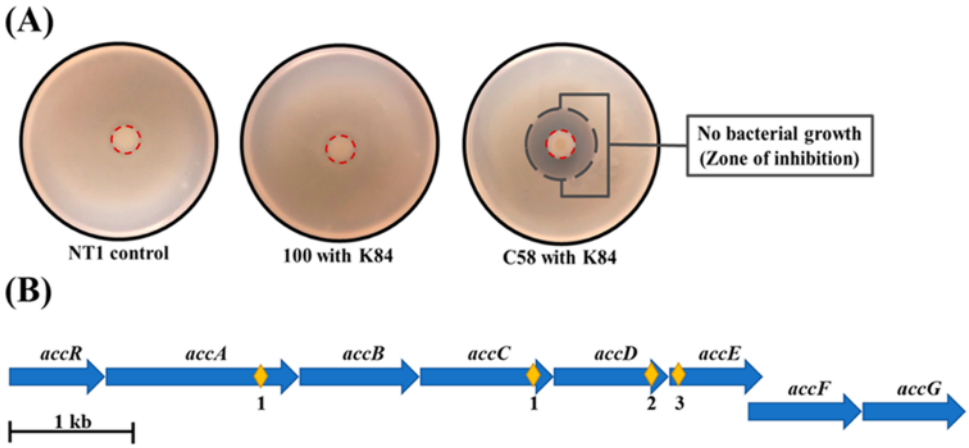

Figure 6. (A) Observations of the agrocin 84 bioassay. As expected, NT1 shows no inhibition when cocultured with K84 and was used as the positive control. The isolated C58 mutant (herein referred to as 100) also shows no inhibition when cocultured with K84, similar to NT1, while C58 bacteria show a clearing (zone of inhibition) surrounding the K84 at the plate center. K84 bacterial growth is contained inside the red dashed line. The boundary of the zone of inhibition, if present, is denoted by the gray dash line. (B) Most agrocin 84 resistant mutants carry mutations in the *acc* operon. The location of the *acc* operon mutations found in seven of the nine isolated mutants is represented with yellow diamonds, with numbers below indicating how many times a mutation in this position was observed. All *acc* mutants were recovered from different agrocin 84 resistant microcolonies. Mutants with identical mutations were recovered from different hydrogels and so cannot be the result of cross-contamination during recovery. Each gene is shown as an arrow, and they all have been drawn to scale.

solution for 72 h; fresh media were added to this solution every 24 h. After 72 h, the media was changed to ATGN only and incubated for an additional 48 h to enable the surviving, agrocin-resistant mutants to fully develop inside the hydrogels (Figure 5Bii). Resistant mutants appeared at a density of 0.057 microcolonies/mm^2 (18 ± 7 resistant mutants per hydrogel). The negative control hydrogel, treated the same way as the test hydrogels, rarely produced microcolonies (<0.0011 microcolonies/mm^2), verifying that parental C58-GFP cells very rarely survived when K84 CFCF was present. At the conclusion of the screen, the total number of rare microcolonies in a representative test hydrogel was 25, representing 0.089% of the cell population. Each rare colony was extracted from this hydrogel, plated, and recovered for genomic analysis; 23/25 microcolonies were successfully recovered.

3.5. Follow-Up Phenotypic and Genotypic Analysis of Rare Cells. Following cell retrieval and recovery, colonies were again streaked onto media containing kanamycin and spectinomycin. To corroborate phenotypic observations in the hydrogel with standard microbiological approaches, the agrocin 84 bioassay was performed as described in Section 2.12.[35,36] For every extracted microcolony, a random subset (n = 5) of recovered colonies that showed resistance to the antibiotics, as well as a set of controls for every isolated mutant (Figure 6A), was tested for agrocin 84 resistance. The coculture of C58 with K84 was included as an agrocin 84 sensitive control for which we expected a zone of inhibition (a region near K84 with no bacterial growth due to inhibition) to form. Additionally, the coculture of *A. tumefaciens* NT1 with K84, a bacterial strain that is known to be resistant to agrocin 84, was used to compare the degree of resistance/susceptibility of the hydrogel isolates. The agrocin 84 bioassay verified successful recovery of 9 resistant mutants. Four of these resistant mutants came from two recovered microcolonies, and we failed to recover resistant mutants from 16 of the 23 recovered microcolonies. These observations validate the agrocin 84 resistant phenotype observed in the hydrogel screen and also demonstrate that results observed in the screen can be corroborated using follow-up tests due to the ability to extract, isolate, and grow colonies of interest from the screening interface.

The final step was to connect the observed phenotype with a genotype of the extracted isolates using whole genome sequencing. Previous work identified that the *acc* operon of the Ti plasmid in C58 encodes for the utilization of agrocinopines A and B and for susceptibility to agrocin 84 with mutations in this region resulting in agrocin 84 resistant phenotypes.[26,47,48] This gave a clear expectation for the location of genotypic mutations that should be present in the mutants isolated from the hydrogels. Whole genome sequence analysis showed that 78% (7/9) of the isolated mutants that were sequenced from the screen had mutations in genes within the *acc* locus (Figure 6B). About 20% of the isolated mutants (2/9) lacked a mutation in the *acc* locus; however, they had mutations in other membrane transporter genes. It has been previously shown that inhibitors like agrocin 84 can enter bacterial cells through these transporters; however, more research is required to determine the genetic basis of agrocin 84 resistance in these mutant strains. Taken together, our observations verify that successful genotype-to-phenotype determinations can be made from rare mutants isolated from the hydrogel screen.

4. CONCLUSIONS

Photodegradable hydrogels have been widely studied as matrices for biological applications due to their biocompatibility, tunable chemical and physical properties, and cross-linking abilities. These materials offer a unique set of advantages for cell screening applications: viable, high density cell encapsulation and monitoring, molecular exchange for cell growth and function, and spatiotemporal control of matrix degradation for cell release and retrieval when a patterned light source is used. While these materials have been developed extensively toward drug delivery and tissue engineering applications and have been successfully used for capture and on-demand release of rare circulating tumor cells,[49] they have largely remained separate from applications in microbiology.

https://dx.doi.org/10.1021/acs.biomac.0c00543
Biomacromolecules XXXX, XXX, XXX−XXX

Here, we demonstrate the use of photodegradable hydrogels for high-throughput screening of bacterial populations. To our knowledge, this is also the first successful use of photodegradable hydrogel materials in a bacterial cell screening application. The novelty of the approach lies in the combination of high-density culture, allowing for parallel, microscopic observation of tens of thousands of cellular microcolonies, followed by sequential sampling of any desired microcolony at high resolution and with high purity, enabling follow-up genetic characterization of a rare or desired phenotype.

Given the pervasive knowledge gap between bacteria phenotype and genotype, we anticipate that this simple, materials-driven approach to screening and isolation will benefit a variety of different screens. The proof-of-principle for ML screening demonstrated here with a simple growth/no growth phenotype lays the foundation for more complex phenotypic screens, such as using fluorescence or colorimetric reporters to screen for mutations disrupting gene regulation,[14] or growth-based screening of auxotrophic mutants that have loss of enzymatic function leading to metabolic deficiencies.[50] Using traditional approaches, these screens typically require observations of tens of thousands of macroscopic colonies in hundreds of agar or agarose plates. This throughput can be matched with a single photodegradable hydrogel when combined with a high-throughput image analysis tool to rapidly identify rare cellular phenotypes.[51] The high-throughput nature of our approach along with its repeatability and fast turnaround time also make this approach applicable to other cell separations in microbiomes, clinical samples, and mammalian cell lines.

■ ASSOCIATED CONTENT

Supporting Information

The Supporting Information is available free of charge at https://pubs.acs.org/doi/10.1021/acs.biomac.0c00543.

PEG-*o*-NB-diacrylate synthesis scheme, ^{1}H NMR spectrum of PEG-*o*-NB-diacrylate; hydrogel preparation procedure scheme; hydrogel thickness optimization to prevent microcolony overlay; hydrogel degradation kinetics; PDMS holder setup for light exposure and cell retrieval process; growth curve of C58 ML; bacteria ability to break down the hydrogel membrane; microscopic images for the comparison of cell release efficiency using different light patterns; relation between microcolony diameter and CFU/mL; strains and plasmids; references (PDF)

Supplementary Movie 1: Real time play back of the extraction of colonies using the ring pattern (40× objective) (MOV)

Supplementary Movie 2: Real time play back of the extraction of cells using the broken cross pattern (10× objective, light intensity = 4.2 mW/mm^2) (MOV)

Supplementary Movie 3: Real time play back of the extraction of cells using the line pattern (10× objective, light intensity = 4.2 mW/mm^2) (MOV)

■ AUTHOR INFORMATION

Corresponding Authors

Ryan R. Hansen − *Tim Taylor Department of Chemical Engineering, Kansas State University, Manhattan, Kansas 66506, United States;* orcid.org/0000-0002-6471-047X; Phone: +1-785-532-0625; Email: rrhansen@ksu.edu

Thomas G. Platt − *Division of Biology, Kansas State University, Manhattan, Kansas 66506, United States;* orcid.org/0000-0003-0082-1127; Phone: +1-785-532-6280; Email: tgplatt@ksu.edu

Authors

Niloufar Fattahi − *Tim Taylor Department of Chemical Engineering, Kansas State University, Manhattan, Kansas 66506, United States*

Priscila A. Nieves-Otero − *Division of Biology, Kansas State University, Manhattan, Kansas 66506, United States*

Mohammadali Masigol − *Tim Taylor Department of Chemical Engineering, Kansas State University, Manhattan, Kansas 66506, United States;* orcid.org/0000-0002-3367-7646

André J. van der Vlies − *Tim Taylor Department of Chemical Engineering, Kansas State University, Manhattan, Kansas 66506, United States*

Reilly S. Jensen − *Division of Biology, Kansas State University, Manhattan, Kansas 66506, United States*

Complete contact information is available at: https://pubs.acs.org/10.1021/acs.biomac.0c00543

Author Contributions

[▽]N.F. and P.A.N.-O. are co-first authors. The manuscript was written through contributions of all authors. All authors have given approval to the final version of the manuscript.

Notes

The authors declare no competing financial interest.

■ ACKNOWLEDGMENTS

This research was supported by the National Science Foundation (Award 1650187). N.F. would like to acknowledge the National Science Foundation Research Trainee Innovations in Food, Energy, and Water Systems (NRT-INFEWS) program (Award 1828571) and support from the Dr. Larry Erickson Fellowship Award (Kansas State University). P.A.N.-O. would like to acknowledge support from the National Science Foundation Graduate Research Fellowship (Award GGVP004842). We would like to thank Christopher Carter for help with the agrocin 84 bioassays. We also thank the Kansas IDeA Networks of Biomedical Research Excellence (K-INBRE) Bioinformatics Core (P20GM103418) for help with using scripts used in the bioinformatic analyses. The computing for this project was performed on the Beocat Research Cluster at Kansas State University, which is funded in part by NSF grants CNS-1006860, EPS-1006860, EPS-0919443, ACI-1440548, CHE-1726332, and NIH P20GM113109.

■ REFERENCES

(1) Ishii, S.; Tago, K.; Senoo, K. Single-Cell Analysis and Isolation for Microbiology and Biotechnology: Methods and Applications. *Appl. Microbiol. Biotechnol.* **2010**, *86* (5), 1281−1292.

(2) Welch, J. D.; Williams, L. A.; DiSalvo, M.; Brandt, A. T.; Marayati, R.; Sims, C. E.; Allbritton, N. L.; Prins, J. F.; Yeh, J. J.; Jones, C. D. Selective Single Cell Isolation for Genomics Using Microraft Arrays. *Nucleic Acids Res.* **2016**, *44* (17), 8292−8301.

(3) Holland, S. L.; Reader, T.; Dyer, P. S.; Avery, S. V. Phenotypic Heterogeneity Is a Selected Trait in Natural Yeast Populations Subject to Environmental Stress. *Environ. Microbiol.* **2014**, *16* (6), 1729−1740.

(4) Huys, G. R.; Raes, J. Go with the Flow or Solitary Confinement: A Look inside the Single-Cell Toolbox for Isolation of Rare and Uncultured Microbes. *Curr. Opin. Microbiol.* **2018**, *44*, 1−8.
(5) Brehm-Stecher, B. F.; Johnson, E. A. Single-Cell Microbiology: Tools, Technologies, and Applications. *Microbiol. Mol. Biol. Rev.* **2004**, *68* (3), 538−559.
(6) Czechowska, K.; Johnson, D. R.; van der Meer, J. R. Use of Flow Cytometric Methods for Single-Cell Analysis in Environmental Microbiology. *Curr. Opin. Microbiol.* **2008**, *11* (3), 205−212.
(7) Faraghat, S. A.; Hoettges, K. F.; Steinbach, M. K.; Van Der Veen, D. R.; Brackenbury, W. J.; Henslee, E. A.; Labeed, F. H.; Hughes, M. P. High-Throughput, Low-Loss, Low-Cost, and Label-Free Cell Separation Using Electrophysiology-Activated Cell Enrichment. *Proc. Natl. Acad. Sci. U. S. A.* **2017**, *114* (18), 4591−4596.
(8) Tatematsu, K.; Kuroda, S. Automated Single-Cell Analysis and Isolation System: A Paradigm Shift in Cell Screening Methods for Bio-Medicines. In *Advances in Experimental Medicine and Biology*; Springer: New York LLC, 2018; Vol. *1068*, pp 7−17; DOI: 10.1007/978-981-13-0502-3_2.
(9) DeMello, A. J. Control and Detection of Chemical Reactions in Microfluidic Systems. *Nature* **2006**, *442* (7101), 394−402.
(10) El-Ali, J.; Sorger, P. K.; Jensen, K. F. Cells on Chips. *Nature* **2006**, *442* (7101), 403−411.
(11) Psaltis, D.; Quake, S. R.; Yang, C. Developing Optofluidic Technology through the Fusion of Microfluidics and Optics. *Nature* **2006**, *442* (7101), 381−386.
(12) Pratt, S. L.; Zath, G. K.; Akiyama, T.; Williamson, K. S.; Franklin, M. J.; Chang, C. B. DropSOAC: Stabilizing Microfluidic Drops for Time-Lapse Quantification of Single-Cell Bacterial Physiology. *Front. Microbiol.* **2019**, *10*, 2112.
(13) Kou, S.; Cheng, D.; Sun, F.; Hsing, I. M. Microfluidics and Microbial Engineering. *Lab Chip* **2016**, *16* (3), 432−446.
(14) Lim, J. W.; Shin, K. S.; Moon, J.; Lee, S. K.; Kim, T. A Microfluidic Platform for High-Throughput Screening of Small Mutant Libraries. *Anal. Chem.* **2016**, *88* (10), 5234−5242.
(15) Nam, S.; Stowers, R.; Lou, J.; Xia, Y.; Chaudhuri, O. Varying PEG Density to Control Stress Relaxation in Alginate-PEG Hydrogels for 3D Cell Culture Studies. *Biomaterials* **2019**, *200*, 15−24.
(16) Kloxin, A. M.; Kasko, A. M.; Salinas, C. N.; Anseth, K. S. Photodegradable Hydrogels for Dynamic Tuning of Physical and Chemical Properties. *Science (Washington, DC, U. S.)* **2009**, *324* (5923), 59−63.
(17) Sergeeva, A.; Vikulina, A. S.; Volodkin, D. Porous Alginate Scaffolds Assembled Using Vaterite CaCO3 Crystals. *Micromachines* **2019**, *10* (6), 357.
(18) Duarte, J. M.; Barbier, I.; Schaerli, Y. Bacterial Microcolonies in Gel Beads for High-Throughput Screening of Libraries in Synthetic Biology. *ACS Synth. Biol.* **2017**, *6* (11), 1988−1995.
(19) Connell, J. L.; Ritschdorff, E. T.; Whiteley, M.; Shear, J. B. 3D Printing of Microscopic Bacterial Communities. *Proc. Natl. Acad. Sci. U. S. A.* **2013**, *110* (46), 18380−18385.
(20) Zengler, K.; Toledo, G.; Rappé, M.; Elkins, J.; Mathur, E. J.; Short, J. M.; Keller, M. Cultivating the Uncultured. *Proc. Natl. Acad. Sci. U. S. A.* **2002**, *99* (24), 15681−15686.
(21) Kloxin, A. M.; Tibbitt, M. W.; Anseth, K. S. Synthesis of Photodegradable Hydrogels as Dynamically Tunable Cell Culture Platforms. *Nat. Protoc.* **2010**, *5* (12), 1867−1887.
(22) Peppas, N. A.; Hilt, J. Z.; Khademhosseini, A.; Langer, R. Hydrogels in Biology and Medicine: From Molecular Principles to Bionanotechnology. *Adv. Mater.* **2006**, *18* (11), 1345−1360.
(23) Van Der Vlies, A. J.; Barua, N.; Nieves-Otero, P. A.; Platt, T. G.; Hansen, R. R. On Demand Release and Retrieval of Bacteria from Microwell Arrays Using Photodegradable Hydrogel Membranes. *ACS Appl. Bio Mater.* **2019**, *2* (1), 266−276.
(24) Tibbitt, M. W.; Kloxin, A. M.; Sawicki, L. A.; Anseth, K. S. Mechanical Properties and Degradation of Chain and Step-Polymerized Photodegradable Hydrogels. *Macromolecules* **2013**, *46* (7), 2785−2792.
(25) Harrison, J.; Studholme, D. J. Recently Published *Streptomyces* Genome Sequences. *Microb. Biotechnol.* **2014**, *7* (5), 373−380.
(26) Reader, J. S.; Ordoukhanian, P. T.; Kim, J. C.; De Crécy-Lagard, V.; Hwang, I.; Farrand, S.; Schimmel, P. Major Biocontrol of Plant Tumors Targets tRNA Synthetase. *Science* **2005**, *309* (5740), 1533.
(27) Holsters, M.; de Waele, D.; Depicker, A.; Messens, E.; van Montagu, M.; Schell, J. Transfection and Transformation of *Agrobacterium tumefaciens*. *Mol. Gen. Genet.* **1978**, *163* (2), 181−187.
(28) Tempe, J.; Petit, A.; Holsters, M.; Montagu, M. v.; Schell, J. Thermosensitive Step Associated with Transfer of the Ti Plasmid during Conjugation: Possible Relation to Transformation in Crown Gall. *Proc. Natl. Acad. Sci. U. S. A.* **1977**, *74* (7), 2848−2849.
(29) Morton, E. R.; Fuqua, C. Genetic Manipulation of *Agrobacterium*. *Curr. Protoc. Microbiol.* **2012**, *25*, 3D.2.1−3D.2.15.
(30) Khire, V. S.; Lee, T. Y.; Bowman, C. N. Surface Modification Using Thiol−Acrylate Conjugate Addition Reactions. *Macromolecules* **2007**, *40* (16), 5669−5677.
(31) Hu, M.; Noda, S.; Okubo, T.; Yamaguchi, Y.; Komiyama, H. Structure and Morphology of Self-Assembled 3-Mercaptopropyltrimethoxysilane Layers on Silicon Oxide. *Appl. Surf. Sci.* **2001**, *181* (3−4), 307−316.
(32) Sprouffske, K.; Wagner, A. Growthcurver: An R Package for Obtaining Interpretable Metrics from Microbial Growth Curves. *BMC Bioinf.* **2016**, *17* (1), 172.
(33) Baldwin, A. D.; Kiick, K. L. Tunable Degradation of Maleimide−Thiol Adducts in Reducing Environments. *Bioconjugate Chem.* **2011**, *22* (10), 1946−1953.
(34) Masigol, M.; Fattahi, N.; Barua, N.; Lokitz, B. S.; Retterer, S. T.; Platt, T. G.; Hansen, R. R. Identification of Critical Surface Parameters Driving Lectin-Mediated Capture of Bacteria from Solution. *Biomacromolecules* **2019**, *20* (7), 2852−2863.
(35) Hayman, G. T.; Farrand, S. K. Characterization and Mapping of the Agrocinopine-Agrocin 84 Locus on the Nopaline Ti Plasmid pTiC58. *J. Bacteriol.* **1988**, *170* (4), 1759−1767.
(36) Hayman, G. T.; Von Bodman, S. B.; Kim, H.; Jiang, P.; Farrand, S. K. Genetic Analysis of the Agrocinopine Catabolic Region of *Agrobacterium tumefaciens* Ti Plasmid pTiC58, Which Encodes Genes Required for Opine and Agrocin 84 Transport. *J. Bacteriol.* **1993**, *175* (17), 5575−5584.
(37) Li, H.; Durbin, R. Fast and Accurate Short Read Alignment with Burrows-Wheeler Transform. *Bioinformatics* **2009**, *25* (14), 1754−1760.
(38) McKenna, A.; Hanna, M.; Banks, E.; Sivachenko, A.; Cibulskis, K.; Kernytsky, A.; Garimella, K.; Altshuler, D.; Gabriel, S.; Daly, M.; DePristo, M. A. The Genome Analysis Toolkit: A MapReduce Framework for Analyzing Next-Generation DNA Sequencing Data. *Genome Res.* **2010**, *20* (9), 1297−1303.
(39) Allardet-Servent, A.; Michaux-Charachon, S.; Jumas-Bilak, E.; Karayan, L.; Ramuz, M. Presence of One Linear and One Circular Chromosome in the *Agrobacterium tumefaciens* C58 Genome. *J. Bacteriol.* **1993**, *175* (24), 7869−7874.
(40) Sambrook, J.; Russell, D. *Molecular Cloning: A Laboratory Manual*, Fourth ed.; Cold Spring Harbor, 2001.
(41) Weber, L. M.; Lopez, C. G.; Anseth, K. S. Effects of PEG Hydrogel Crosslinking Density on Protein Diffusion and Encapsulated Islet Survival and Function. *J. Biomed. Mater. Res., Part A* **2009**, *90A* (3), 720−729.
(42) Canal, T.; Peppas, N. A. Correlation between Mesh Size and Equilibrium Degree of Swelling of Polymeric Networks. *J. Biomed. Mater. Res.* **1989**, *23* (10), 1183−1193.
(43) Zustiak, S. P.; Leach, J. B. Hydrolytically Degradable Poly(Ethylene Glycol) Hydrogel Scaffolds with Tunable Degradation and Mechanical Properties. *Biomacromolecules* **2010**, *11* (5), 1348−1357.
(44) Metters, A.; Hubbell, J. Network Formation and Degradation Behavior of Hydrogels Formed by Michael-Type Addition Reactions. *Biomacromolecules* **2005**, *6* (1), 290−301.

https://dx.doi.org/10.1021/acs.biomac.0c00543
Biomacromolecules XXXX, XXX, XXX−XXX

(45) Khan, A. H.; Cook, J. K.; Wortmann, W. J.; Kersker, N. D.; Rao, A.; Pojman, J. A.; Melvin, A. T. Synthesis and Characterization of Thiol-Acrylate Hydrogels Using a Base-Catalyzed Michael Addition for 3D Cell Culture Applications. *J. Biomed. Mater. Res., Part B* **2020**, *108* (5), 2294−2307.
(46) Rastogi, R. P.; Richa; Kumar, A.; Tyagi, M. B.; Sinha, R. P. Molecular Mechanisms of Ultraviolet Radiation-Induced DNA Damage and Repair. *J. Nucleic Acids* **2010**, *2010*, 592980.
(47) Hayman, G. T.; Farrand, S. K. *Agrobacterium* Plasmids Encode Structurally and Functionally Different Loci for Catabolism of Agrocinopine-Type Opines. *Mol. Gen. Genet.* **1990**, *223* (3), 465−473.
(48) Kim, H.; Farrand, S. K. Characterization of the *acc* Operon from the Nopaline-Type Ti Plasmid pTiC58, Which Encodes Utilization of Agrocinopines A and B and Susceptibility to Agrocin 84. *J. Bacteriol.* **1997**, *179* (23), 7559−7572.
(49) LeValley, P. J.; Tibbitt, M. W.; Noren, B.; Kharkar, P.; Kloxin, A. M.; Anseth, K. S.; Toner, M.; Oakey, J. Immunofunctional Photodegradable Poly(Ethylene Glycol) Hydrogel Surfaces for the Capture and Release of Rare Cells. *Colloids Surf., B* **2019**, *174*, 483−492.
(50) Connon, S. A.; Giovannoni, S. J. High-Throughput Methods for Culturing Microorganisms in Very-Low-Nutrient Media Yield Diverse New Marine Isolates. *Appl. Environ. Microbiol.* **2002**, *68* (8), 3878−3885.
(51) Jung, J. H.; Lee, J. E. Real-Time Bacterial Microcolony Counting Using On-Chip Microscopy. *Sci. Rep.* **2016**, *6*, 21473.

https://dx.doi.org/10.1021/acs.biomac.0c00543
Biomacromolecules XXXX, XXX, XXX−XXX